# TMT Adaptive Secondary Mirror conceptual design

Biasi Roberto*[a], Mauro Manetti[a], Gerald Angerer[a], Matteo Tintori[b], Daniele Gallieni[b],
Corinne Boyer[c], Lianqui Wang[c], Melissa Trubey[c], Gelys Trancho[c], John Rogers[c]
[a]Microgate Srl, via Waltraud Gebert Deeg, 3e – 39100 Bolzano-Bozen (BZ) – Italy;
[b]A.D.S. International Srl, via Pio Galli sindacalista, 3 – 23841 Annone di Brianza (LC) – Italy;
[c]TMT International Observatory, 100 West Walnut Street, Suite 300 – Pasadena, CA 91124

## ABSTRACT

AdOptica has been contracted in late 2017 to perform a conceptual design for an adaptive secondary mirror for TMT. The proposed solution is based on the large, contactless, voice-coil based adaptive mirror technology already successfully implemented on several 6 to 8m class telescopes and currently in construction for the E-ELT M4 and in final design for the GMT secondary.

The proposed solution for the 3.06m adaptive mirror is based on a Silicon Carbide structural open-back reference body and seven segments for the thin shell, a hexagonal central one and six surrounding segments. Both the reference body surface and the shell segments front and rear surfaces are aspherical. The mirror is controlled by 3828 contactless voice-coil motors with capacitive sensors. The embedded control electronics is mostly installed on the reference body rear side. The design is compatible with the carbon dioxide direct expansion cooling system planned as telescope cooling facility. The conceptual design comprehends also the M2 positioner, based on the classical Steward Platform configuration.

We performed a comprehensive static and dynamic performance analysis, taking into account also reliability and safety aspects. The results indicate that the proposed design meets the TMT requirements.

**Keywords:** TMT, TMT adaptive M2, adaptive mirror, mirror shell, voice-coil

## 1. INTRODUCTION

The TMT adaptive secondary mirror is intended to serve the 2nd generation instruments of the TMT, by replacing the conventional secondary mirror adopted for first light. In this paper we present the conceptual study of the adaptive mirror, performed by AdOptica, a consortium of Microgate and ADS International, in late 2017 and 2018.

The main goals of the adaptive M2 are summarized hereafter:

- Enable Ground Layer AO (GLAO) for TMT first light seeing limited instrument, WFOS (400nm to 1000nm).
- Reduce emissivity for Mid IR AO (MIRAO) instrument (3 to 25 microns)
- Eliminate the requirement for additional large-stroke, low order “woofer” deformable Mirrors in Extreme AO, Multi Object AO, and the NFIRAOS upgrade.
- Provide insurance against higher telescope windshake or more ground layer turbulence.
- Enable Laser Tomography AO for HROS.

The mirror is based on the well consolidated large, contactless deformable mirror concept already deployed on several telescopes, including MMT, LBT, Magellan and VLT. The design has been adapted to the specific case of the TMT M2. Considering the very large size of the unit, with 3.06m diameter, several concepts previously conceived for the ELT M4 adaptive unit [4], currently in advanced construction phase [1], have been adopted also for the TMT AM2. We refer in particular to the structural reference body made of Silicon Carbide and to the shell segmentation, adopted mainly to reduce the manufacturing and operational risks related to the thin shells.

# 2. OPTOMECHANICAL DESIGN

The optomechanical design of the TMT adaptive secondary follows a scheme already adopted for the E-ELT M4: the reference body, which provides a stable reference for the contactless control of the thin shells, has also the structural function of carrying the load of the control actuators and related electronics. The main characteristics of the optomechanical design are summarized in Table 2-1.

To achieve the required structural performance, the reference body is a monolithic structure of Silicon Carbide with a front skin and stiffening ribs with a triangular pattern. The adaptive mirror is made of a segmented thin shell, with one hexagonal central segment and six surrounding petals. The central segment is constrained in-plane by a central membrane and tangential anti-torsional flexures, while the lateral ones are constrained by radial membranes glued along the outer edges. The actuators are uniformly distributed on the mirror surface with a triangular pattern and 50mm pitch, which has been optimized on base of the wavefront residual requirements.

The structural reference body is kinematically mounted on a large aluminum cell, which embeds also the mounting flanges for the positioning hexapod. The upper flanges are mounted directly on the telescope top-end. The hexapod is arranged in a classical Steward Platform configuration and features flexure joints for a frictionless positioning and tracking capability. Figure 2-1Figure 2-2Figure 2-3 provides an overview of the system main components, together with the mounting concept of the unit on the telescope. The large mirror mass imposes high capacity and the stringent stability requirements impose high actuator stiffness. All these features have been already proven in similar applications.

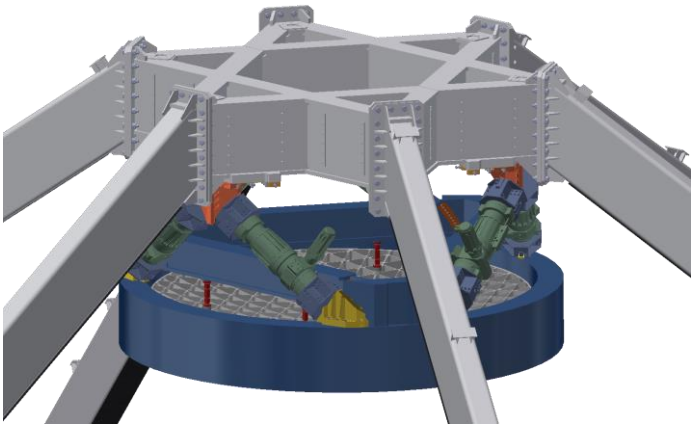

Figure 2-1 - Top-end structure with the adaptive secondary unit.

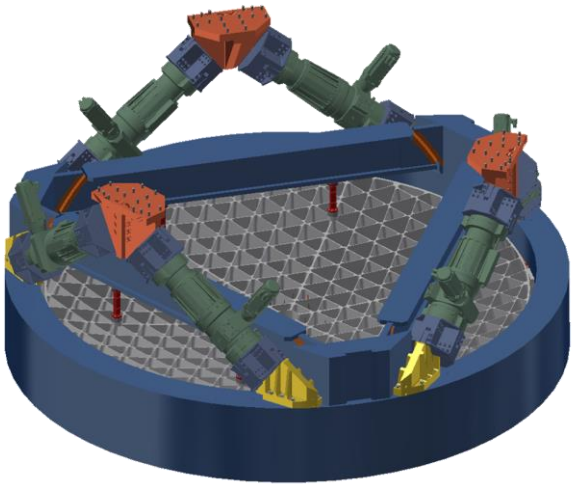

Figure 2-2. Reference body cell and positioner.

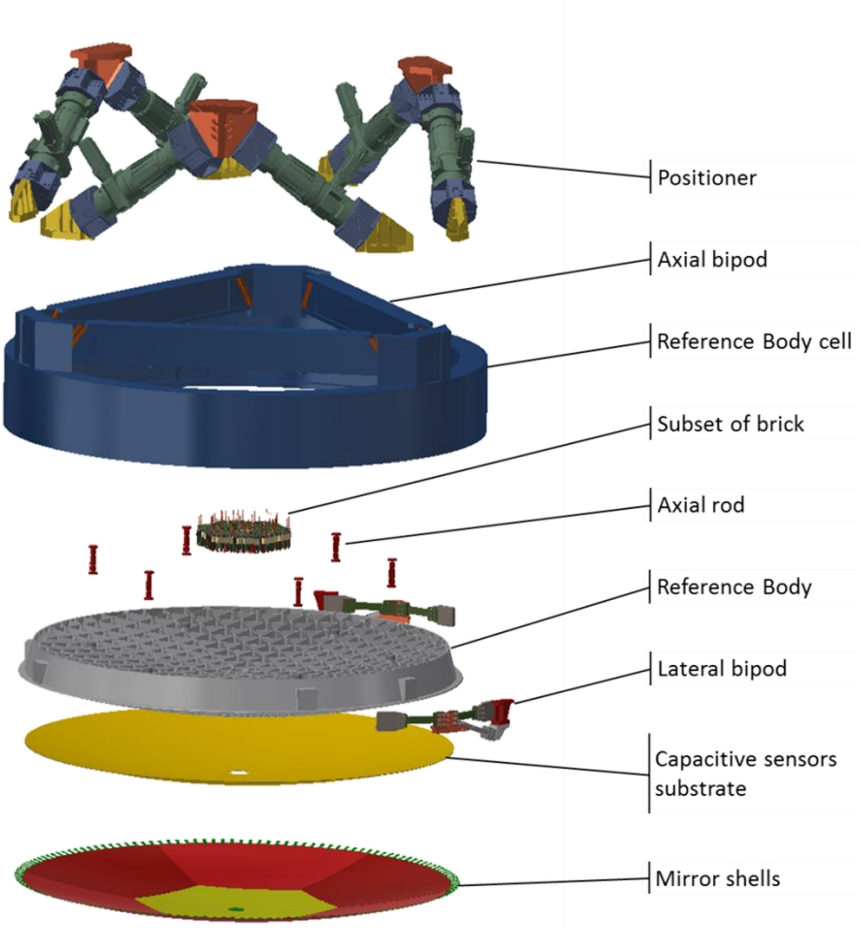


Figure 2-3. Exploded view of the Adaptive Secondary unit.

Table 2-1 - Optomechanical main characteristics.

| | |
|---|---|
| **Mirror shape** | **Convex, r = -6.228m, k = -1.318** |
| **Optical diameter** | **External: 3045.5 mm, internal: 220 mm** |
| **Mechanical diameter** | **External: 3230 mm, internal: 120 mm** |
| **Shell thickness** | **2.9 mm** |
| **Shell material** | **Zerodur** |
| **Shell segmentation** | **1 central + 6 external segments** |
| **Number of VCM actuators** | **Total 3828, 714 on central segment + 6 · 519 on external segments** |
| **Actuators pitch** | **50mm** |
| **Reference body** | **Ribbed open-back structure made of Silicon Carbide** |
| **Reference body cell** | **Aluminum structure, kinematic suspension of the reference body** |
| **Positioner** | **Hexapod** |
| **Total mass** | **~ 8500 kg** |
| **Overall dimensions with positioner** | **Φ = 3600 mm, h = 1600 mm** |

# 3. CONTROL SYSTEM ARCHITECTURE

The control of the TMT adaptive secondary is based on the large, contactless, Voice-Coil actuated adaptive mirror concept already implemented on MMT, LBT, Magellan, VLT, in final design for GMT and in advanced construction for the E-ELT M4.

The TMT AM2 control system comprehends four main subsystems, following their physical location in the telescope:

- AM2 top-end embedded control electronics, comprehending all the electronics and electromechanical devices embedded either directly on the AM2 reference body and on the top-end structure. These components are the 'core' of the control system and implement all functions related to the shell operation, including local and global control, safety and housekeeping;
- M2 CS cabinet located on the elevation platform, containing the power supply units for the embedded electronics, the emergency batteries and the positioner control rack;
- Control, test and calibration unit, based on a standard workstation located in the telescope control room and accomplishing the non-real-time control tasks like system state machine control, maintenance, test and calibration functions;
- Direct expansion gas cooling control system, controlling the 'evaporator' of the $CO_2$-based cooling system, i.e. the accurate cooling of the AM2 top-end embedded electronics; it is also physically located at the AM2 in the available volume of the top-end structure.

The block diagram of the control system architecture is reported in Figure 3-1.

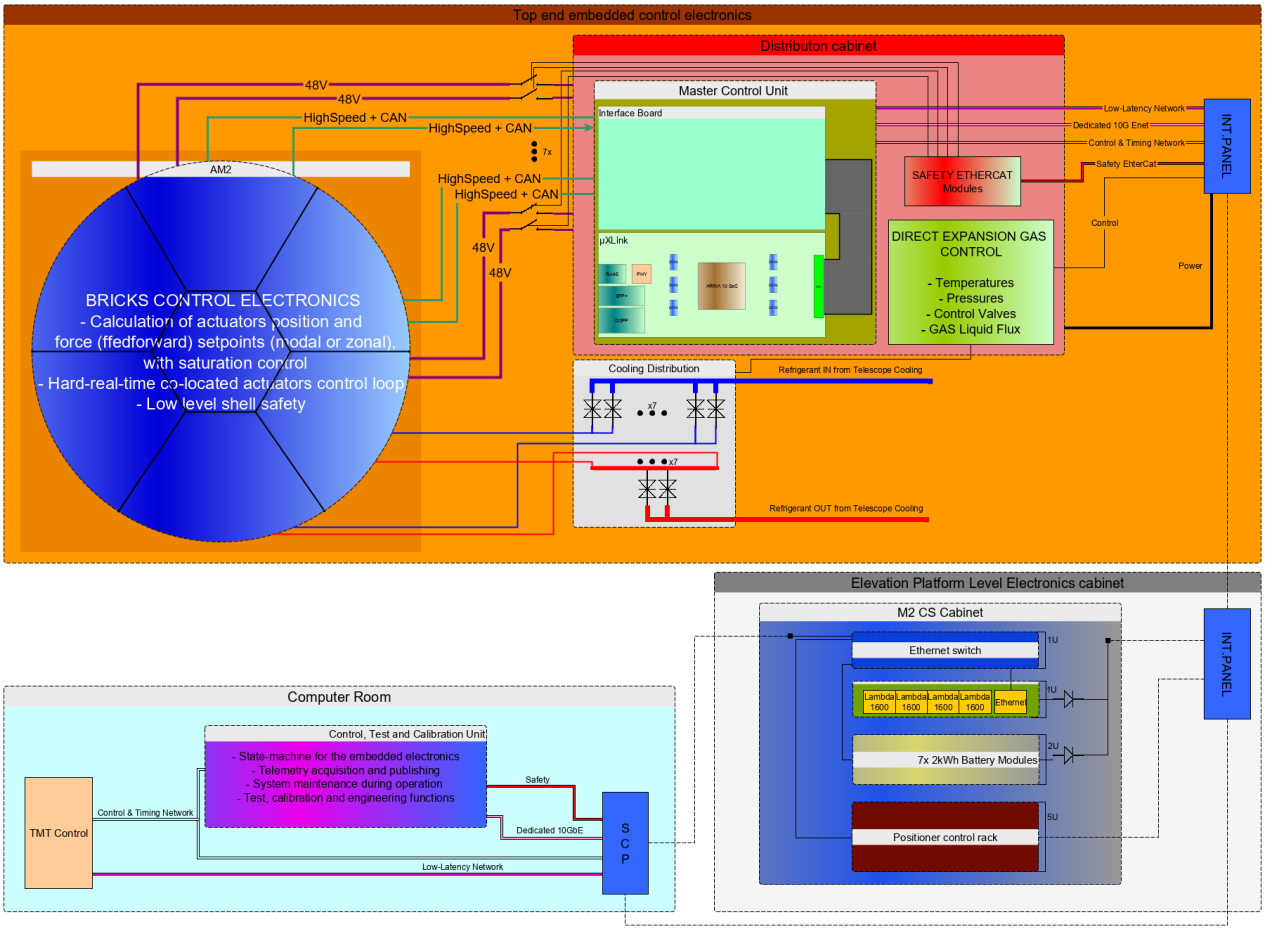


Figure 3-1. Control system block diagram.

### 3.1 Top-end embedded electronics layout

The top end embedded electronics, performing the real-time closed loop control of the adaptive mirror segments, has been specifically tailored to the reference body and cooling design.

The actuators are grouped in bricks, which are aluminum plates typically hosting 6 or 10 actuators each. The reference body cells are populated with such small bricks, each tailored to the cell size.

The bricks are permanently mounted on the reference body, together with the cooling piping, see Figure 3-2. This solution has been chosen to reduce dramatically the number of fittings and quick connectors of the cooling plant, considering also the high operating pressure of the $CO_2$-based cooling system. The actuators can be easily removed from the reference body front face, when the shell is dismounted. On the top of the bricks, the distribution board allows connecting the actuators to the control boards, which are mounted on a flange, cooled by the same cooling circuit, fixed to the reference body ribs - see Figure 3-2. The boards are easily accessible and replaceable in case of failure.

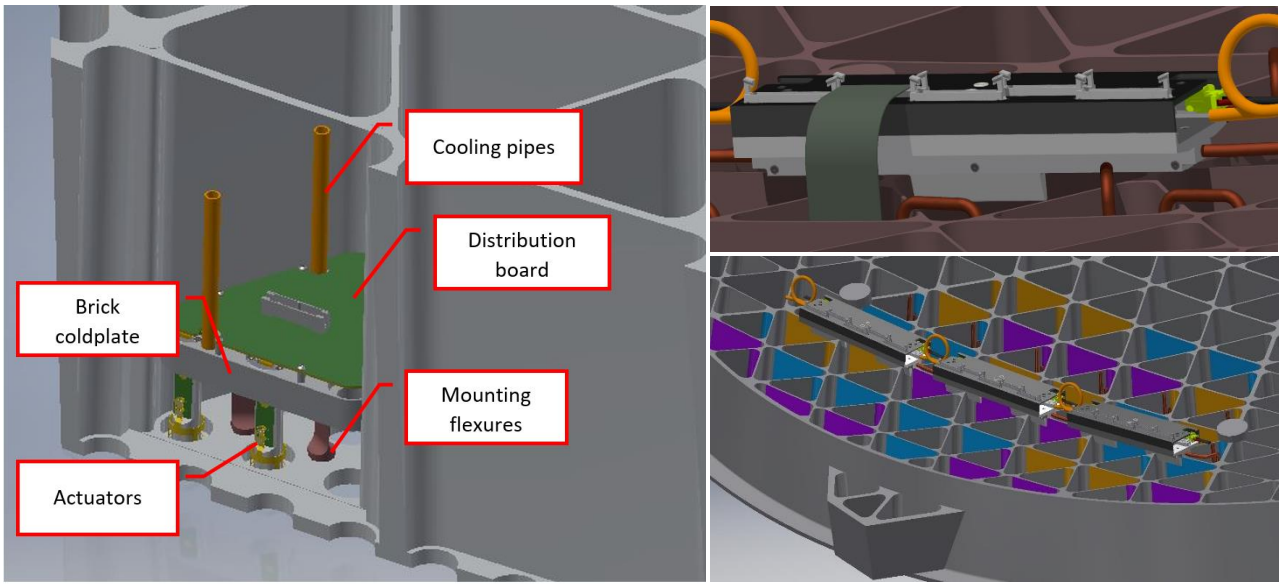


Figure 3-2. Actuators' support bricks (left) and control boards (right).

## 4. OPTICAL CALIBRATION CONCEPT

The optical calibration concept considers two types of tests, one based on an interferometry, the other on optical profilometry.

- Within the **interferometric** test, we considered at feasibility level two different options:
    - **Hindle sphere test**, in which the convex hyperboloidal mirror is tested in double pass from the far focus of the hyperbola, accessing the near focus through a spherical mirror with a central hole; its center of curvature coincides with the near focus of the hyperbola. The interferometer is placed at the far focus of the convex surface
    - **Centre of curvature test**, based on the same concept adopted for the VLT DSM calibration on ASSiST. This test setup requires a large concave aspherical mirror, with an approximate diameter of 5m to cover the whole adaptive mirror
- The **profilometry** test is based on a large number, > 100, of high accuracy absolute distance measurement devices (e.g. the Etalon Absolute Multiline system). The fiber collimators of the measurement system are mounted on a very stable 'fiber plate' having approximately the same radius of curvature of the adaptive mirror.

The profilometry concept, although not being used yet for optical calibration, is very appealing for the lower cost w.r.t the interferometric solution.

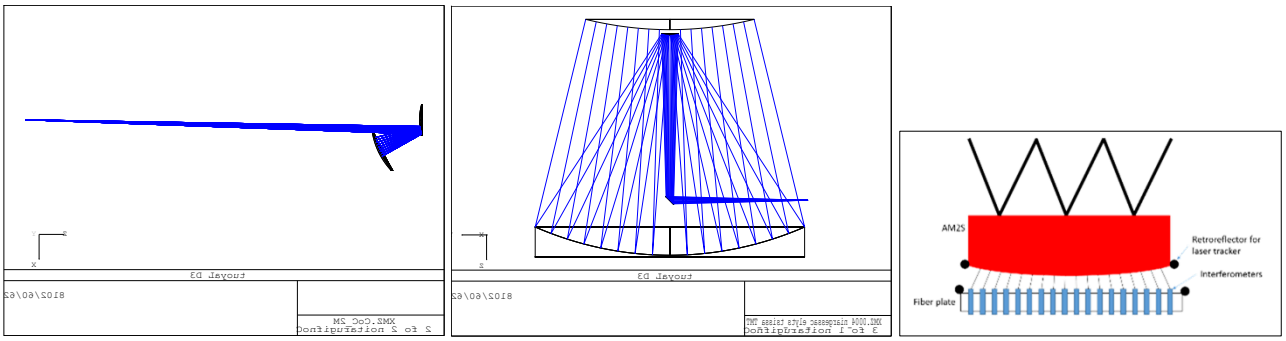


Figure 4-1. From left to right: Hindle sphere test, Center of Curvature test, Profilometer-based test.

# 5. ANALYSIS AND RESULTS

In the frame of the conceptual study, we performed a quite thorough analysis activity comprehending:

- Spherical vs. aspherical mirror shells back surface tradeoff
- Shell thickness preliminary optimization
- Reference body design preliminary optimization
- Fitting error analysis for different seeing conditions, including performance loss due to actuators fault
- Optical surface figure error under gravity, thermal and wind loads
- Actuators stroke and force budget
- Power consumption analysis for different seeing conditions
- Mirror dynamic response and tracking performance analysis with a Hi-Fi multi-physics simulator
- Structural analysis of the whole unit, including positioner, considering gravity, thermal and earthquake loads
- Dynamic structural analysis (eigenmodes)

When relevant, the analysis has been performed considering both the Mauna Kea (MK) and the Observatorio del Roque de Los Muchachos (ORM) sites.

Table 5-1 reports the performance results obtained by simulating 1000 uncorrelated phase screens generated through the superposition of two turbulent layers uncorrelated in space; the mirror shells model includes the influence functions of the actuators to determine the actual fitting error; force saturation is also considered and properly managed by a specific force clipping algorithm, which intervenes very occasionally only in bad seeing conditions.

Table 5-1 - Main performance results, referring to MK and ORM sites.

| Parameter | Units | MK median | ORM median | Bad |
|---|---|---|---|---|
| **$r_0$** | mm | 186 | 178 | 100 |
| **$L_0$** | m | 30 | 30 | 60 |
| **Fitting error without failed acts** | nm RMS | 83 | 86 | 139 |
| **Fitting error limit requirement** | nm RMS | 85.15 | 88.07 | 140.29 |
| **Fitting error with 40 failed acts** | nm RMS | 84 | 87 | 140 |
| **max PtV actuator displacement** | µm | 7.3 | 7.5 | 19.7 |
| **max RMS actuator displacement** | µm RMS | 1.8 | 1.9 | 7.5 |
| **max peak actuator force** | N | 1.35 | 1.292 | 2.146 |
| **mean actuator force** | N | 0 | 0 | 0 |
| **RMS actuator force** | N RMS | 0.251 | 0.262 | 0.423 |

The simulations performed include also the analysis of performance degradation in case of failed actuators, both randomly distributed – see Figure 5-1 - and clustered; the clustered failure is very unlikely but must be considered to take into account the possibility of failure of a control board or distribution board. It shall be noticed that both these subsystems are Line Replaceable Unit, which could be easily replaced, in case of failure, during daytime maintenance.

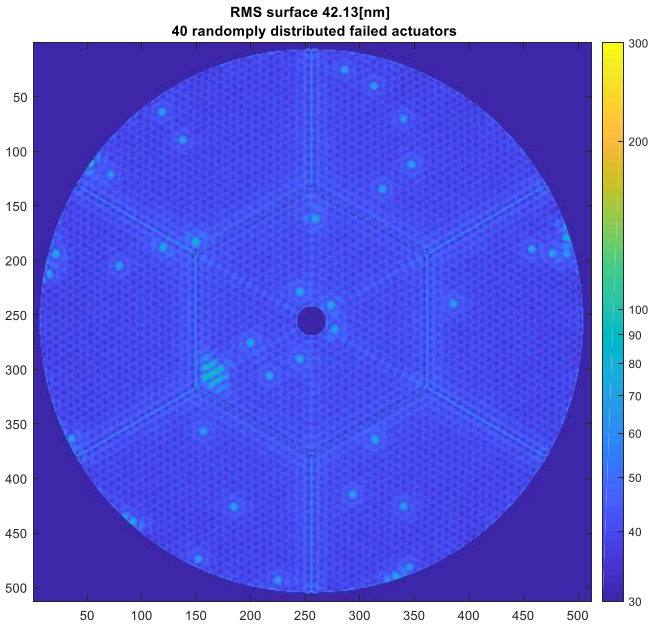


Figure 5-1. Mauna Kea WFE (in time), 40 dead actuators randomly distributed.

In the frame of the conceptual study, we simulated also the effect on the reference body shape of quasi-static disturbances, in particular gravity, thermal and wind dynamic pressure. Figure 5-2 presents two results related to gravity, in which the

error is computed as difference from the zenith-pointing reference case, and to maximum wind expected in operating conditions.

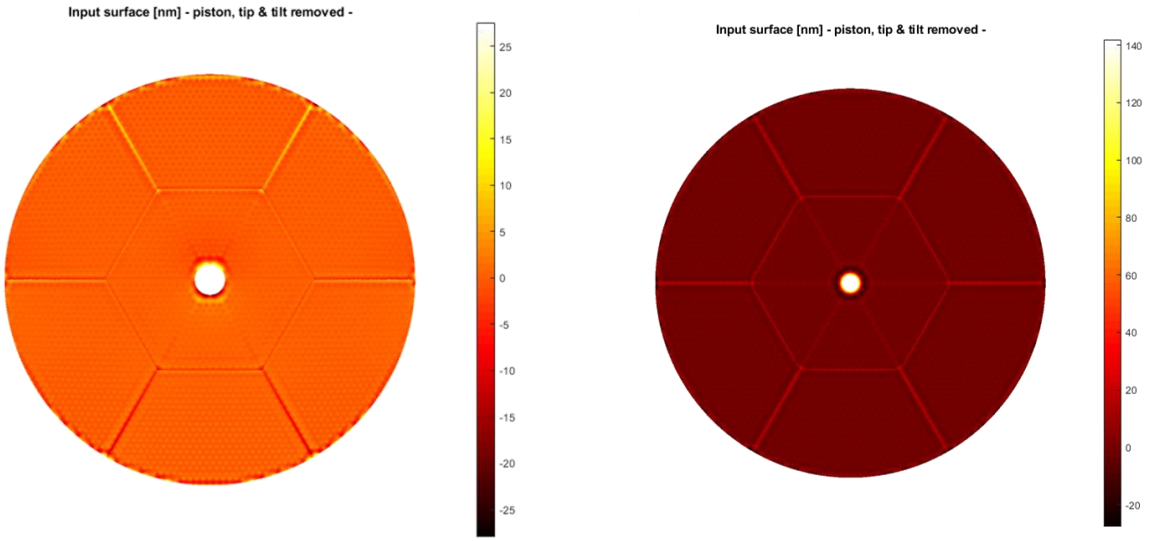


Figure 5-2. Mirror shape for the horizon pointing case (left) and with 9.7 $ms^{-1}$ wind load (right).

An additional important simulation case relates to the dynamic performance of the mirror, which has been studied using the high-fidelity numerical simulation tool specifically developed for that, which considers the elastic model of the shell, the shell control system and the fluid-dynamic effect of the air trapped in the gap between shell and reference body [2][3]. This numerical tool allows assessing the system stability and dynamic response, providing a dynamic description of the mirror behavior that can be potentially exploited for the assessment of the optical loop performance. Some typical result of a turbulence time history and a modal step response are shown in Figure 5-3.

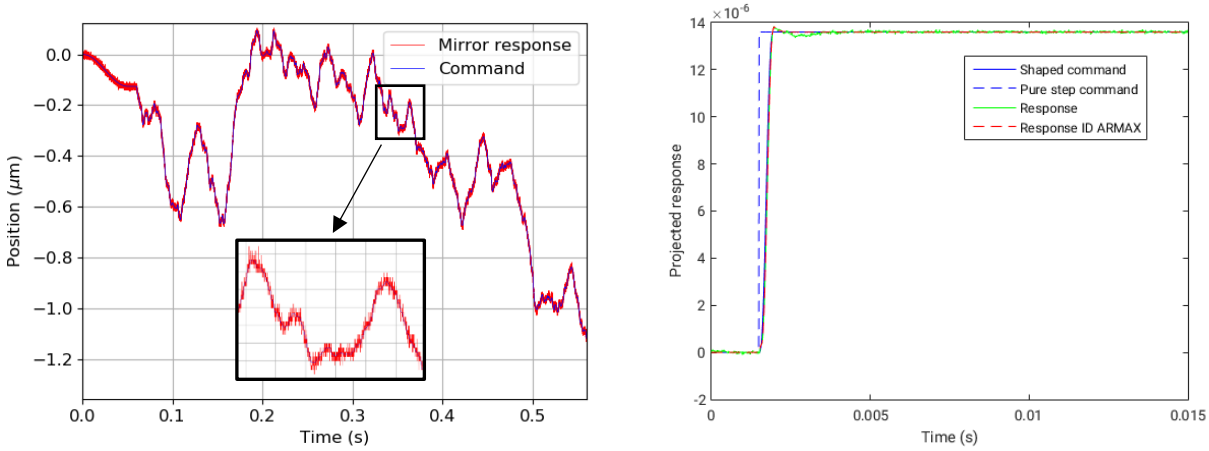


Figure 5-3. Left: time response of one actuator, median seeing @ MK. Tracking error is 7nm RMS WF.
Right: time response of one actuator and ARMAX-identified equivalent SISO model response

## 6. FINAL REMARKS

The TMT Adaptive Secondary design has been developed to a sufficient level to demonstrate that it meets the system requirements in terms of performance, reliability and maintainability. The activity comprehended also the development of a design and MAIT plan, including ROM costing and survey with the vendors of the most critical items, namely reference body and thin shells, to confirm that those part are actually manufacturable within a defined time frame.

## REFERENCES


[1] Vernet, E., Biasi, R., Gallieni. D. et al, “Building the ESO ELT M4 adaptive unit”, in this conference

[2] Manetti, M., Morandini, M., Mantegazza, P., “Servo-Fluid-Elastic Modeling of Contactless Levitated Adaptive Secondary”, Computational Mechanics 50 (1), 85-98 (2012).

[3] Manetti, M., Morandini, M., Mantegazza, P., Biasi, R., Gallieni, D., Riccardi, A., “Modeling and control of massively actuated, magnetically levitated, adaptive mirrors” In IEEE international conference on control applications (CCA) (pp. 860–866) (2010).

[4] Gallieni, D., Tintori, M., Mantegazza, M., Anaclerio, E., Crimella, L., Acerboni, M., Biasi, R., Angerer, G., Andrigettoni, M., Merler, A., Veronese, D., Carel, J.-L., Marque, G., Molinari, E., Tresoldi, D., Toso, G., Spanó, P., Riva, M., Mazzoleni, R., Riccardi, A., Mantegazza, P., Manetti, M., Morandini, M., Vernet, E., Hubin, N., Jochum, L., Madec, P., Dimmler, M., Koch, F., ”Voice-coil technology for the E-ELT M4 Adaptive Unit”, Presented at the Adaptative Optics for Extremely Large Telescopes, (2010).